Optical and Quantum Electronics (2022) 54:588
https://doi.org/10.1007/s11082-022-03990-4

B_2O_3/PbO/Na_2O/MgO/Nb_2O_5 glasses: fabrication, physical, optical characteristics as well as photons/neutrons/beta particles attenuation capacities

Norah A. M. Alsaif[1] · Y. S. Rammah[2] · I. O. Olarinoye[3] · Emad M. Ahmed[4] · A. S. Abouhaswa[2,5]

Received: 12 May 2022 / Accepted: 10 July 2022 / Published online: 3 August 2022

Abstract
Physical, optical characteristics, and radiation attenuation capacities of the prepared (50-x) $B_2O_3 + 30PbO + 10Na_2O + 10MgO + xNb_2O_5$ glasses with various doping ratios x = 0, 2, 4, 6, and 8 mol% have been investigated. Glasses were prepared using the well-known melt quenching process and named as their corresponding x value. The density and molar volume of the prepared glasses were increased from 4.71 g/cm^3 and 23.76 cm^3/mol for the sample with free Nb_2O_5 to 4.91 g/cm^3 and 25.99 cm^3/mol for the rich sample with x = 8 mol% of Nb_2O_5. With increasing Nb_2O_5 concentration, the broad near-visible band centered was moved towards higher wavelength. The direct band gap energies of glass samples felt from 3.728 to 2.939 eV, while the indirect band gap energies from 3.032 to 1.822 eV as the Nb_2O_5 substitution ratio increased. Urbach's energies of the prepared samples were increased with the increasing of Nb_2O_5. For photons, the maximum values of mass attenuation coefficient (MAC) were 32.67, 33.02, 33.38, 33.74, and 34.10 cm^2/g for x = 0 – x = 8, respectively at 0.015 MeV, while the least corresponding MAC value of 0.0286, 0.0288, 0.0291, 0.0293, and 0.0295 cm^2/g was obtained at 10 MeV. For neutrons, the fast $(MAC)_{FN}$ was decreased from 0.0185 – 0.0161 cm^2/g, while the thermal $(MAC)_{TN}$ was decayed from 6.6538 – 5.5903 cm^2/g. Analysis of the TSP and CSDA range of the glasses emphasize the fact that there is no significant difference in the charged particle of the glasses irrespective of the weight fraction of Nb_2O_5 relative B_2O_3. Results confirm that the current glasses are superior for radiation shielding materials compared to some commercial concrete and glasses.

Keywords Glasses · Optical properties · Photons · Neutron attenuation

✉ Y. S. Rammah
dr_yasser1974@yahoo.com

Extended author information available on the last page of the article

1 Introduction

Glass is a class of materials whose applications have evolved over the years. In modern times, the application of glasses includes: optical, electronic, communication, and radiation shielding applications amongst others. In shielding functionality, the choice of glasses has progressed due to the need of transparent, cheap, chemically stable, mechanically strong, thermally stable, high radiation resistant and absorption prowess materials. The ease at which a glass chemical architecture can be altered to produce different physical, chemical, and radiation shielding property combinations is a major point of attraction that has made glass shields popular in radiation protection technology.

Recently, it is observed that borate based glasses are potential materials for the optical devices and optical fibre industry because of their high visible and infrared (IR) transparencies (Ersundu et al. 2012; Sabry and El-Samanoudy 1995; Upender and Prasad 2017). In addition, these glasses have good chemical and thermal stability, high values of nonlinear refractive index (Sabry and El-Samanoudy 1995; Upender and Prasad 2017; Cardinal et al. 1996). Adding niobium (V) to borate based glasses possess a wide range of infrared and nonlinear optical response (Cardinal et al. 1996). Therefore these glasses can be applied in various applications in optical filters, optical memory devices, IR domes, and laser windows (Cardinal et al. 1996; Flambard et al. 2008; Nowak et al. 2013). There are several numbers of reports over preparation, thermal, structure, and optical features of various borate, phosphate, tellurite, and silicate glasses with participation of Nb_2O_5, they reported that the presence of Nb_2O_5 in the glass network improves their optical properties (Upender and Prasad 2017; Cardinal et al. 1996; Flambard et al. 2008; Nowak et al. 2013; Shams et al. 2020; Koudelka et al. 2016; Marcondes et al. 2018).

Today many glass species with different brand names are commercially available for radiation protection application. Many more based on experimental data have shown potentially better performance than existing shields and have been suggested as alternative shielding materials (Rammah et al. 2021a, 2021b; Al-Buriahi et al. 2021; Sekhar et al. 2021; Abouhaswa et al. 2021). In most occasions, it is the dense and heavy metals (such as Pb, Bi, W, Ba, Mo, etc.) containing glasses/ glasses containing higher proportion of these elements that have shown better photon and charged particle shielding prowess (Sekhar et al. 2021; Rammah et al. 2021b; Abouhaswa et al. 2021). Recently investigated Pb-based glasses have shown outstanding potentials in terms of radiation shielding parameters for shielding applications (Abouhaswa et al. 2021; Al-Harbi et al. 2021; Almuqrin et al. 2021). Lately, Al-Harbi and colleagues (Al-Harbi et al. 2021) investigated the role of PbO content in the radiation shielding capacity of P_2O_5–CaO–Na_2O–K_2O–PbO glass structure. It was concluded that higher Pb content in the glass system reduced photon transmission. Also, the increase in the Pb content of PbO-WO_3-Na_2O-MgO-B_2O_3 glasses led to a significant improvement in the mass density, photon and electron shielding ability of the glasses (Almuqrin et al. 2021). Furthermore, the PbO–WO_3–Na_2O–MgO–B_2O_3 glasses had superior photon absorption ability when compared to common shields such as ordinary concrete, and steel magnetite concrete (Bashter 1997). The positive influence of Pb on the radiation shielding ability of other glass structures have been identified (Abouhaswa et al. 2021). In the quest to produce more sophisticated glass shields with outstanding radiation shielding abilities, physical and chemical properties that could fit into existing and future radiation protection applications, many glass systems are at different experimental stages of radiation

shielding investigations. Some of these glasses could become reliable future alternative materials in nuclear technology applications.

As shown formerly, glasses containing Nb_2O_5 characterized with an excellent transmittance in the visible and near infrared regions; therefore these glasses have high potential for practical applications in variety of optical devices. In addition, insertion of Nb_2O_5 with high density (4.6 g/cm^3) in the glass composition leads to increase the density of glasses and improves their capacity as radiation shielding materials. Therefore, in this study, we fabricate and investigate the optical properties, photon, beta particle, fast and thermal neutron attenuation parameters of (50-x)B_2O_3 + 30PbO + 10Na_2O + 10MgO + xNb_2O_5 glasses with the view of establishing for the first time their suitability for shielding applications. Boron (B) has a high cross section for thermal and fast neutrons while the cross section of photons and energetic charged particles is high in Pb, hence, the combination of B and Pb in the glass chemical structure suggests potentially good shielding effectiveness for these radiations. This serves as part of the motivation for this investigation. Data and conclusions from this study would be of great interest to radiation protection scientists and engineers who are constantly seeking alternative glass materials for shielding and other applications in nuclear science and technology. To this end, the major aim of this work is to investigate the physical and optical properties of the prepared B_2O_3/PbO/Na_2O/MgO/Nb_2O_5 glasses. Also, photons, neutrons, and beta particles attenuation characteristics of the studied glasses have been examined.

2 Experimental technique and methods

2.1 Samples preparation

Five glass samples with nominal compositions of (50-x)B_2O_3 + 30PbO + 10Na_2O + 10MgO + xNb_2O_5 were prepared using the well-known melt quenching process with various doping ratios x = 0, 2, 4, 6, 8 mol%. To ensure a uniform combination of the glass samples, boron oxide (B_2O_3), lead oxide (PbO), sodium oxide (Na_2O), magnesium oxide (MgO), and niobium pentoxide (Nb_2O_5) powders were carefully blended. Subsequently the combinations were poured into a porcelain crucible and melted at 1080˚C for 30 min before being suddenly shaped into a stainless-steel pattern to shape the glass samples into discs. The melting glass samples were quenched in the mold and annealed at 300˚C for 3 h before cooling to room temperature.

Archimedes' rule was used to determine the densities of the glasses, and the dipping fluid was toluene, which has a density of 0.86 g/cm^3. Table 1 illustrates the density and molar volume of the manufactured glass samples.

To investigate the optical absorption of polished glass samples, Cary 5000 UV–Vis–NIR double beam spectrophotometer (wavelengths range from 200 to 3000 nm) has been used.

2.2 Radiation attenuation

The photon, neutron, and beta particle shielding parameters of (50-x)B_2O_3 + 30PbO + 10Na_2O + 10MgO + xNb_2O_5 glasses with x = 0, 2, 4, 6, 8 and coded as x = 0, 2, 4, 6, and 8 were investigated and obtained theoretically. The glasses were prepared with the traditional melt-quench method. The chemical composition, density, molar volume, and molecular weight of the glasses detailed in Table 1. In order to evaluate the photon,

Table 1 Samples code, chemical composition, density, and molar volume for prepared glass samples

Samples code	Chemical composition mol%					Density g/cm^3 ± 0.01	Molar volume (cm^3/mol) ± 0.01
	B_2O_3	PbO	Na_2O	MgO	Nb_2O_5		
x = 0	50	30	10	10	0	4.71	23.76
x = 2	48	30	10	10	2	4.76	24.31
x = 4	46	30	10	10	4	4.80	24.93
x = 6	44	30	10	10	6	4.84	25.52
x = 8	42	30	10	10	8	4.91	25.99

neutron (fast and thermal), and beta-particle attenuation parameters, the WinXCOM (Gerward et al. 2001), NGCal (Gökçe et al. 2021) and ESTAR (Berger et al. 1999) were adopted. These theoretical tools are a reliable and faster way of evaluating shielding parameters for these radiation species. More so, theoretical calculations of radiation interaction parameters are cost effective and eliminate the possible radiation exposure to the investigator(s). The mass attenuation coefficients of the glasses were estimated for photon energies E in the range $0.15 \leq E \leq 15$ MeV via the mixture rule (Almuqrin et al. 2021) in WinXCOM platform with the chemical specification of each glass as indicated in Table 1 used as input parameters. Also, the thermal (25 MeV) and fast neutron (4 MeV) mass attenuation capacity of the glasses were determined with the application of a new and free online NGCal software while the stopping power and range of electrons with energies in the range $0.10 \leq E \leq 10$ MeV were estimated in SRIM. These parameters were analyzed in order to ascertain the shielding efficacy of these glasses against these radiations.

3 Results and discussion

3.1 Density and molar volume

The density and molar volume of the $(50\text{-}x)B_2O_3 + 30PbO + 10Na_2O + 10MgO + xNb_2O_5$ glass samples system as a function of Nb_2O_5 concentration are displayed in Fig. 1. As shown in Fig. 1 and Table 1, with the increasing substitution ratio of Nb_2O_5 content (x) in the glass composition, the density and molar volume of samples were increased. The increasing of glass density from 4.71 g/cm^3 for the sample with free of Nb_2O_5 to 4.91 g/cm^3 for the sample with enrich with Nb_2O_5. This gradual increase of density may be attributed to the addition of niobium which cause modifying in the network of glass samples by filling the interstitial spaces with the higher molecular weight (265.81 g/mol) and density (4.6 g/cm^3) of Nb_2O_5 than molecular weight (69.62 g/mol) and density (2.46 g/cm^3) of B_2O_3. The gradual increase in the molar volume of the prepared glasses from 23.76 to 25.99 cm^3/mol can be attributed to that atomic radius of niobium atom (207 pm) is larger than that of boron atom (192 pm), which leads to change in the bond length inside the glass network and cause an increase in molar volume.

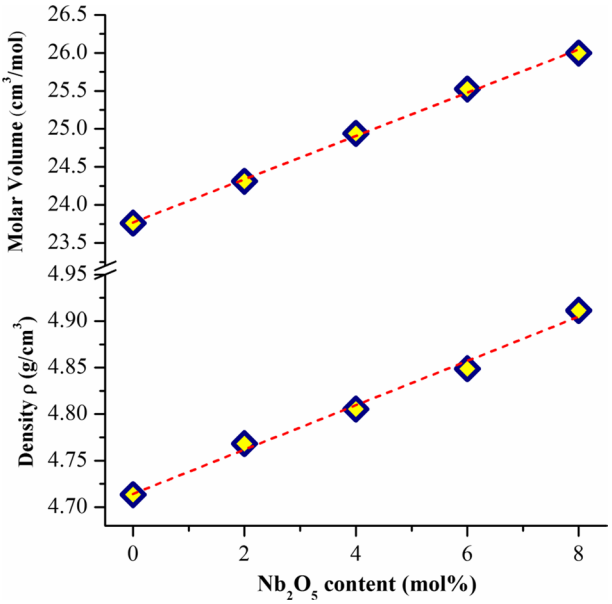

Fig. 1 Density and molar volume of the prepared Nb-x glass samples

3.2 Optical properties

Figure 2a shows the UV–visible absorption spectra of (50-x)B_2O_3 + 30PbO + 10Na_2O + 10 MgO + xNb_2O_5 glass samples doped with Nb_2O_5. With increasing Nb_2O_5 substitution concentration, the absorbance of samples improved significantly. For the undoped sample, the spectrum displays a broad near-visible band centered at around 355 nm. With increasing Nb_2O_5 concentration, the broad near-visible band centered moved towards higher wavelength 445 nm. This means that by increasing Nb_2O_5 concentration in the prepared glasses, the cut off wavelength was shifted to higher wavelength; therefore, the optical energy band gap will be reduced with increasing Nb_2O_5 content in glasses (Upender and Prasad 2017; Shams et al. 2020). The absorption coefficient was also estimated using the equation $\alpha = \frac{2.303A}{t}$ where A is the absorption and t is glass samples thickness. By increasing substitution concentration of Nb_2O_5 doped in the glasses, the absorption coefficient has been improved and shifted towards higher wavelengths (redshift), as seen in Fig. 2b.

Tauc's rule, which was modified by Mott and Davis, was used to estimate the optical energy band gaps for the investigated glass samples doped with Nb_2O_5 as in Eq. (1) (Davis and Mott 1970; Abouhaswa et al. 2018);

$$(\alpha h\nu)^m = C\left(h\nu - E_g\right) \tag{1}$$

where hν is the energy of the incident photon and C is a constant. The power (m) represents the kind of electronic transition, with m = 2 and 1/2 indicating a direct and indirect allowable transition, respectively. Using m = 2 and plots of $(\alpha h\nu)^2$ vs. hν, the direct band gap energies for the prepared glass samples can be estimated by extrapolating the linear section using the straight line until intersect the hν-axis as shown in Fig. 3a. The predicted direct band gap energy of glass samples felt from 3.728 to 2.939 eV as the Nb_2O_5 substitution ratio increased. In order to get the values of indirect band gap, m = 1/2 is applied in

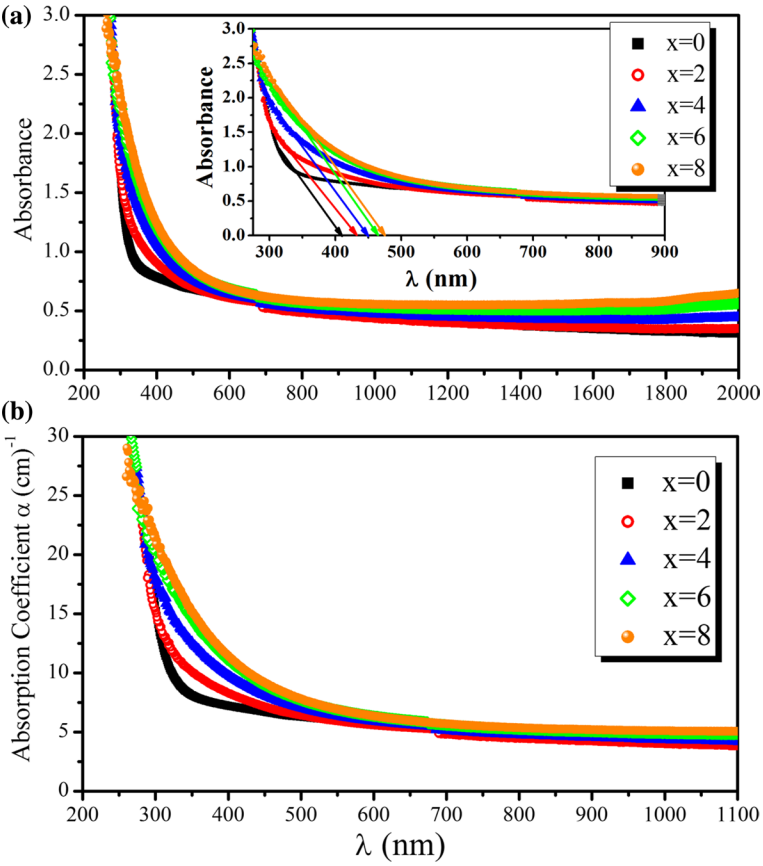

Fig. 2 **a** UV–visible absorption spectrum, **b** the absorption coefficient of glass samples doped with Nb_2O_5

Eq. (1) and plotting the variation of $(\alpha h\nu)^{1/2}$ as a function of $(h\nu)$ as displayed in Fig. 3b as shown in Fig. 3b, the indirect band gap energy decreased from 3.032 to 1.822 eV as the Nb_2O_5 concentration increased in the prepared glasses.

Urbach's empirical formula describes the relationship between the absorption coefficient (α) and photon energy (hν) as expressed in given Eq. (2) (Urbach 1953):

$$\alpha = \alpha_0 \exp\left(\frac{h\nu}{E_u}\right) \tag{2}$$

where α_o and E_u represent to Urbach's energy. Equation (2) can be written as expressed in Eq. (3):

$$\ln\alpha = \ln\alpha_0 + \left(\frac{h\nu}{E_u}\right) \tag{3}$$

As a result, Urbach's energy (E_u) may be determined from the slope of the straight line obtained by plotting ln(α) versus (hν). The E_u values are given in Fig. 4; the findings reveal that when the Nb_2O_5 concentration increased, the Urbach's energies

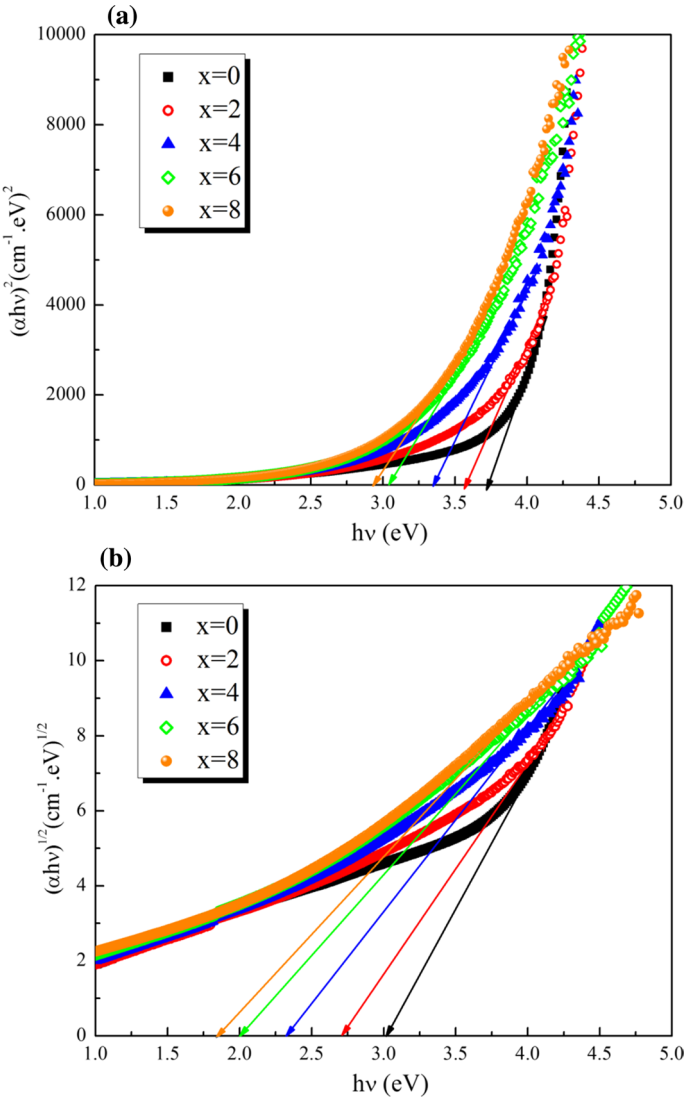

Fig. 3 The dependence of $(\alpha h\nu)^2$ and $(\alpha h\nu)^{1/2}$ on $(h\nu)$ for direct and indirect transitions for examined glass

increased, indicating less stability and homogeneity materials with more defects, as well as an increase in disorder in the produced glass samples.Values of direct, indirect optical band gaps, and Urbach's energy of the proposed glasses are collected as a function of Nb_2O_5 concentration and displayed in Fig. 4. The obtained results are in agreement with previous reports (Upender and Prasad 2017; Shams et al. 2020). For the prepared glasses, Fig. 5 shows the dependence of ln(α) on the photon energy (hν).

The following Eq. (4) can be used to compute the extinction coefficient (k) (Abouhaswa et al. 2019):

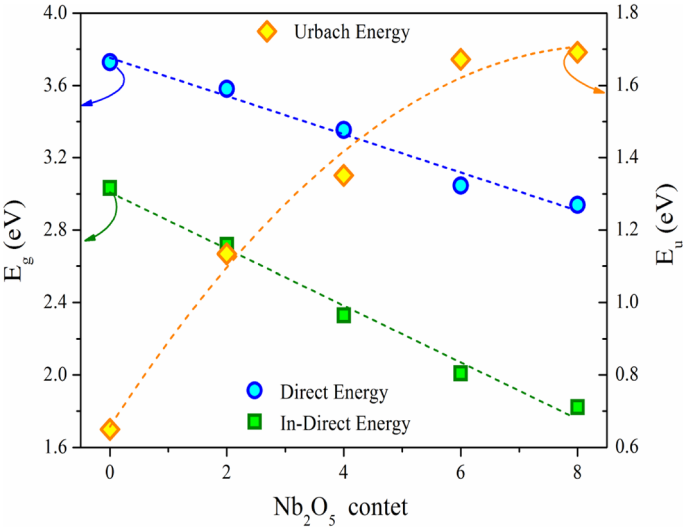

Fig. 4 Dependence of energy gap and Urbach energy on Nb_2O_5 content for prepared glass samples

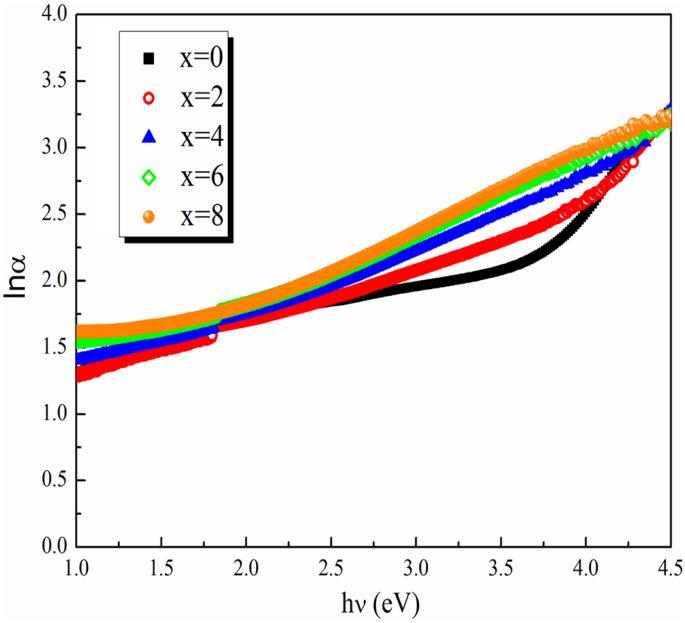

Fig. 5 Dependence of ln(α) on the photon energy (hυ) for prepared glasses

$$k = \frac{\alpha\lambda}{4\pi} \tag{4}$$

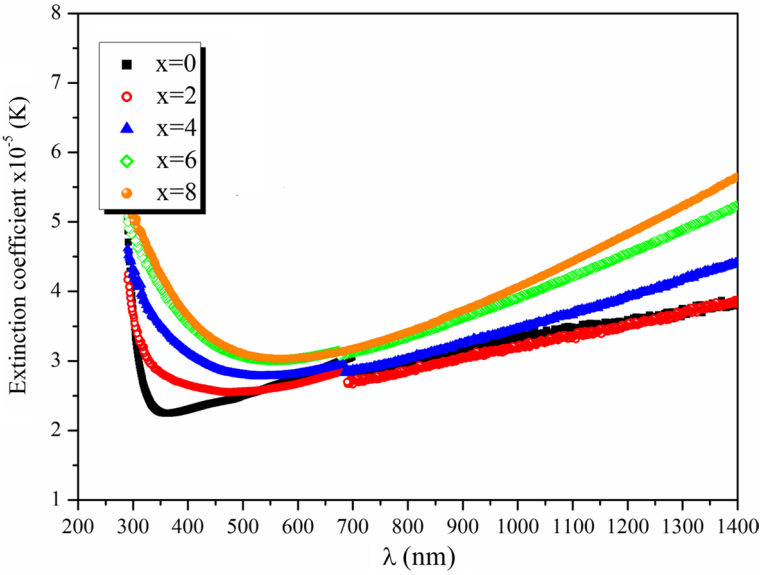

Fig. 6 Dependence of excitation coefficient at different wavelengths for prepared glasses

The dependence of k for prepared glass samples at different wavelengths is seen in Fig. 6. The extinction coefficient was increased with increase Nb_2O_5 substitution ratio.

Fig. 7 MAC versus photon energy for the glasses

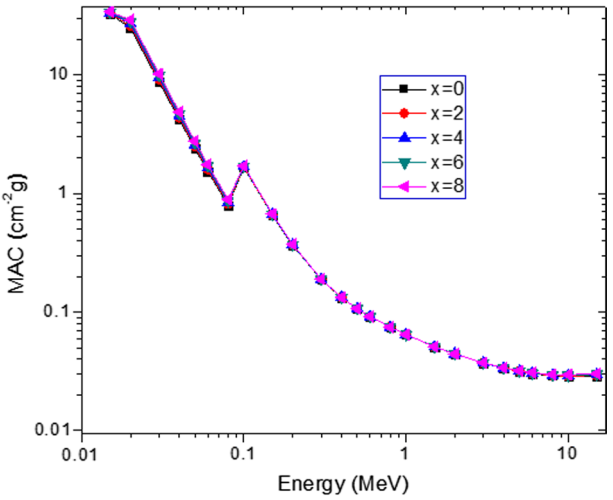

3.3 Radiation attenuation parameters

3.3.1 Photons

The value of mass attenuation coefficient MAC of the glass system and its variation with photon energy is presented in Fig. 7. MAC obviously declines with energy smoothly except at 0.1 and 15 MeV. The sharp rise in MAC value at 0.1 MeV is basically due to the K-absorption edge of the Pb atom. High photoelectric absorption at the K- absorption edge is responsible for the high MAC value at this energy. Such peaks have been recorded for other glasses containing Pb (Abouhaswa et al. 2019) Maximum MAC value of 32.67, 33.02, 33.38, 33.74, and 34.10 cm^2/g were recorded for x = 0 – x = 8, respectively at 0.015 MeV, while the least corresponding MAC value of 0.0286, 0.0288, 0.0291, 0.0293, and 0.0295 cm^2/g was obtained at 10 MeV. The behavior of MAC with respect to energy is attributed to photoelectric effect PE, Compton scattering Cs, and pair production PP partial photon interaction cross sections σ variations with energy. As shown in Fig. 7, the MAC values of the prepared glasses suffered an exponential reduction with the incident photon energy due to the photoelectric effect (PE) interaction in low energy spectrum zone ($0.015 \leq E \leq 0.6$ MeV) in which $\sigma_{PE} \propto E^{-3.5}$. In the medium energy zone ($0.6 \leq E \leq 10$ MeV), MAC values decreased linearly associated with an increase in the Compton scattering interaction (CS), where $\sigma_{CS} \propto E^{-1}$. In the high energy zone, the MAC values are approximately constant; this can be attributed to the pair production cross-section $\sigma_{PP} \propto E^{-2}$.

The effect of the increase of Nb_2O_5 content with respect to B_2O_3 on the photon absorption efficiency of the glasses is shown in Fig. 8. The figure presents the variation of the linear attenuation coefficient $LAC = MAC \times \rho$ as a function of E. although the variation of MAC with respect to E is similar to that of LAC as expected, however, the difference

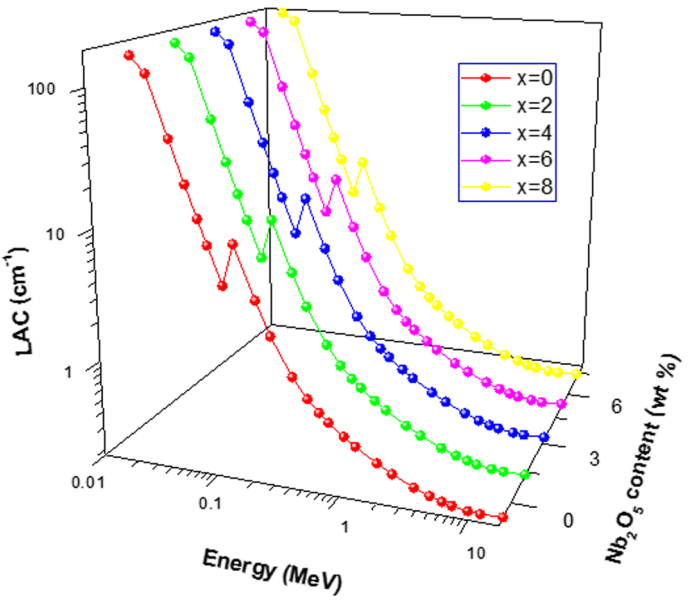

Fig. 8 Influence of Nb_2O_5 content of the glasses on the glasses' LAC values

in the LAC value of the glasses at specific energies is more significant to that MAC. This is due to MAC being normalized for density (ρ) while LAC is normalized for thickness of the glasses. The close proximity in the density explains the strong overlapping in MAC values at nearly all energies as seen in Fig. 7. Maximum and least values of LAC obtained at 15 keV and 10 MeV corresponds to 154 and 0.134; 157.49 and 0.138; 160.43 and 0.140; 163.60 and 0.142; and 167.51 and 0.145 cm^{-1} for x = 0 – x = 8, accordingly. Clearly, the partial replacement of B_2O_3 with Nb_2O_5 improved the photon absorption capacities of the glasses.

The effective atomic number Z_{eff} is another parameter that could be used to analyze the photon shielding ability of a given material. It is strongly dependent on E and chemical composition of the said material. It can be obtained directly from MAC values according to the expression (Mahmoud et al. 2021; Rammah et al. 2021c):

$$Z_{eff} = \frac{\sum_i f_i A_i (MAC)_i}{\sum_i f_j \frac{A_i}{Z_i} (MAC)_i} \tag{5}$$

The variation of Z_{eff} of the present glasses with photon E is depicted in Fig. 9. According to the figure, Z_{eff} initially increases with E up to Pb K-absorption edge but thereafter declines in value with E. Z_{eff} value varies from 10.18 – 32.05 with maximum (minimum) value obtained 0. 1 and 1.5 MeV. At Pb absorption edge, Z_{eff} = 30.45, 30.70, 30.96, 31.55, and 32.05 for x = 0 – x = 8, accordingly. Clearly, the photon absorption capacity trend of the glasses is such that: x = 0 < x = 2 < x = 4 < x = 6 < x = 8; similar to both LAC and MAC. High PE absorption ($\sigma_{PE} \propto Z^4$) is responsible for higher at PE dominant energies while the decline and later rise of Z_{eff} can be attributed to $\sigma_{CS} \propto Z$ and $\sigma_{PP} \propto Z^2$. Also the increase in the value of Z_{eff} as Nb_2O_5 weight fraction increases in the glasses can be attributed to higher atomic number Z of Nb compared to B. Z_{eff} always increase when weight fraction of higher Z atoms increase in a composite material (Manohara et al. 2008; Olarinoye

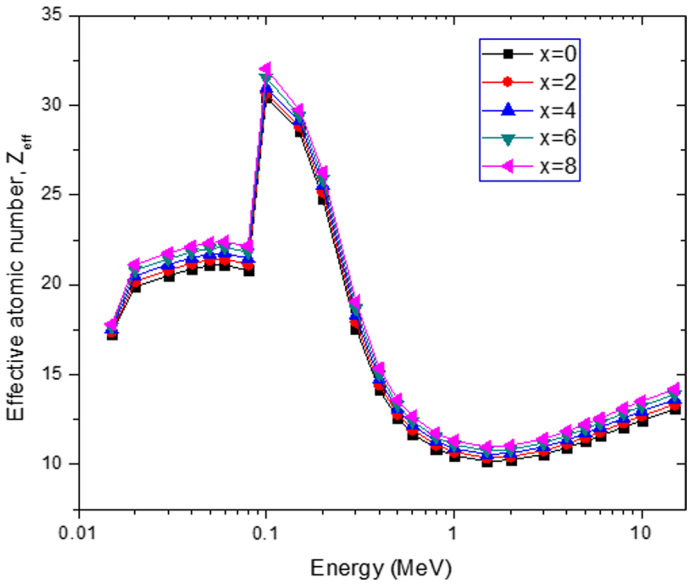

Fig. 9 Effective atomic number and its variation with energy for the investigated glasses

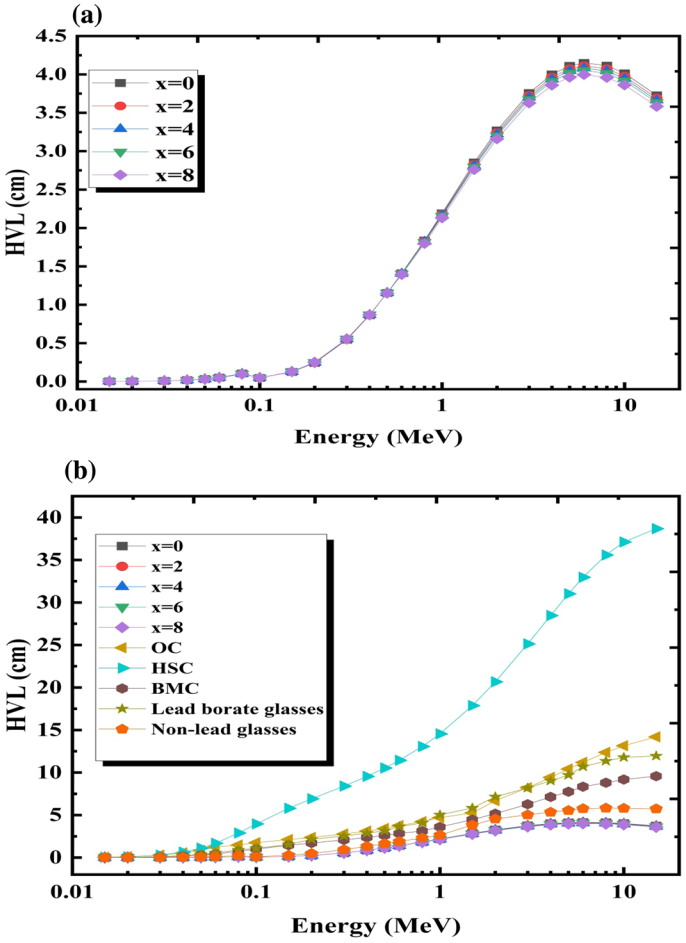

Fig. 10 **a** HVL of the prepared glasses and **b** HVL compared with some concrete, lead borate glasses, and non-lead glasses at different photon energies

2011). Hence, the addition of Nb_2O_5 in the glass matrix improves its photon shielding competence.

In order to position the present glasses as potential shields in contemporary nuclear energy facilities, their half-value layer (HVL) was calculated via Phy-X/PSD software (Şakar et al. 2020). The variation of HVL of the prepared glasses as a function of photon energy is displayed in Fig. 10a. From this Figure, it is observed that the sample with x = 8 mol% of Nb2O5 has the smallest HVL, therefore it can be considered as superior for radiation shielding among all other current glasses. Values of HVL of the present glasses compared with those of known commercial radiation shields such as Ordinary concrete (OC) (Bashter 1997), Hematite-Serpentine concrete (HSC) (Bashter 1997), Basalt-Magnetite concrete (BMC) (Bashter 1997), lead borate glasses (Singh and Badiger 2015), and non-lead glasses (Singh et al. 2014) as shown in Fig. 10b. Figure 10b indicates that HVL of the prepared glasses are lower than those of OC, HSC, BMC, some lead and non-lead borate glasses. Therefore the suggested glasses in the current work are better photon absorbers

compared to other materials i.e., the current glasses show good potential to replace these materials in shielding applications.

So far the photon interaction parameters evaluated and analyzed are those of narrow beam (good) geometry. In a bad geometry situation, buildup factors B are used to relatively compare the photon shielding materials. B measures the level of scattered photons and also the creation of secondary photons within the glass media. Such scattered and secondary photons eventually penetrate the glass and hence reduce its shielding capacity. Detailed discussion about B can be found in the literature (Harima 1993; Olarinoye et al. 2019). The exposure B (EBUF) and energy absorption B (EABUF) of the glasses were estimated via the well-known EXABCal software (Olarinoye et al. 2019) for $0.015 \leq E \leq 15$ MeV for selected depth within 40 MFP. Figures 11 and 12 represent the energy spectrum EABUF and EBUF of $X=0$ and $X=8$, respectively at selected depths. The buildup factors vary similarly for all the glasses; lowest in the PE dominated energies, highest at the CS dominated energies. The high buildup factors at CS dominated energies can be attributed the multiple photon scattering at these energies due to CS while the low values at PE energies is due to complete photon absorption due to photoelectric absorption. High EABUF and EBUF at Pb K-absorption edge is due to de-excitation of excited atoms as a result of K-absorption. To relate the ability of the glasses to transmit scattered photons, EBUF and EABUF of the glasses were compared at three selected energies and presented in Figs. 13, 14 and 15. The buildup factors increase with depth at all energies as a result of multiple photon scattering at high depths. Also, there appears to be no significant differences in the EABUF and EBUF at lower energies due to similarity in the chemical composition of the glasses. However, at greater depth and energy the buildup factors increase as Nb_2O_5 content grows in the glasses.

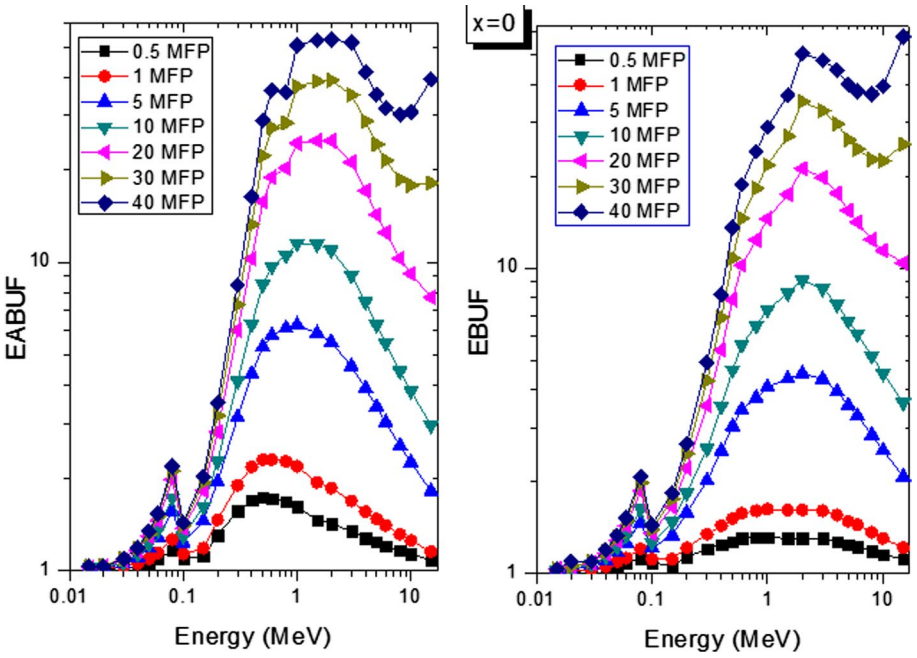

Fig. 11 Spectrum of EABUF and EBUF of $x=0$ at selected depths

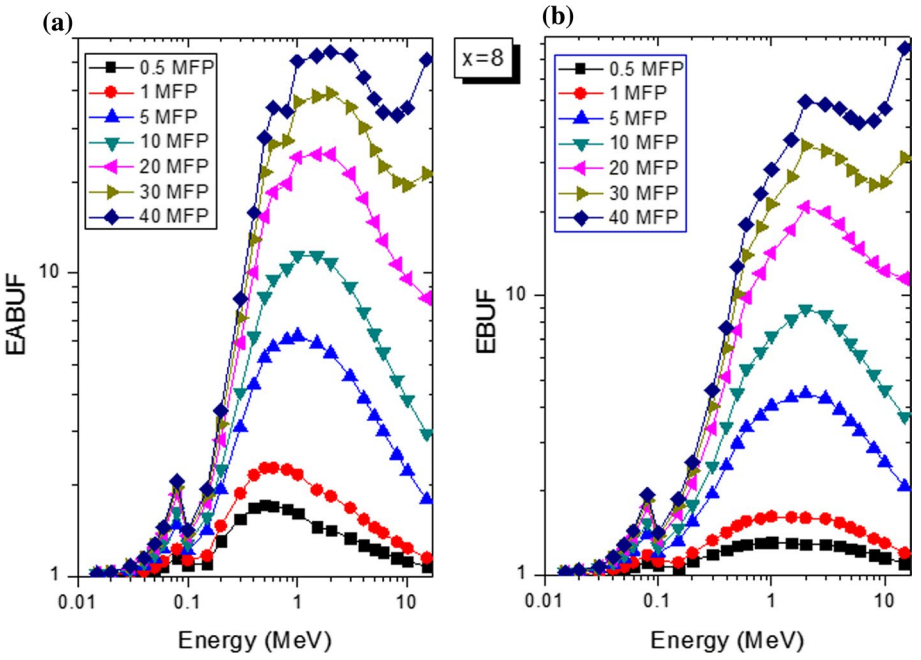

Fig. 12 Spectrum of EABUF and EBUF of x = 8 at selected depths

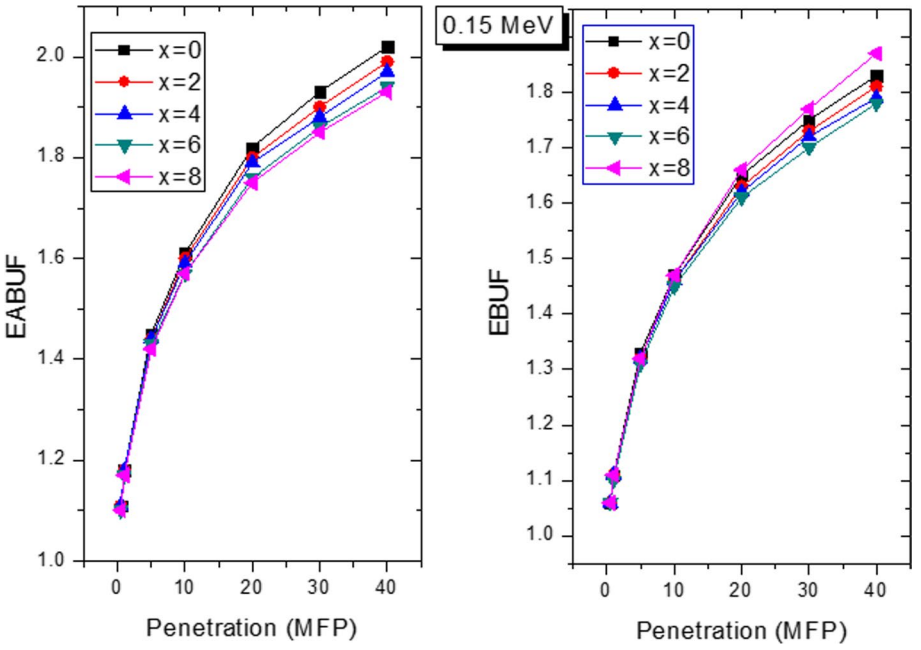

Fig. 13 EABUF and EBUF as a function of depth at 0.15 MeV for the glasses

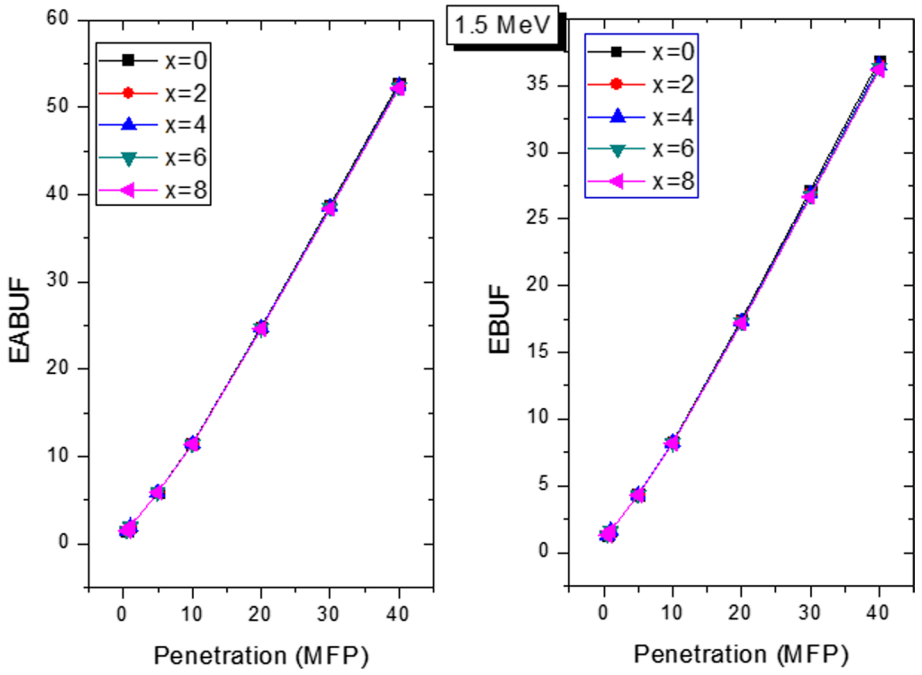

Fig. 14 EABUF and EBUF as a function of depth at 1.5 MeV for the glasses

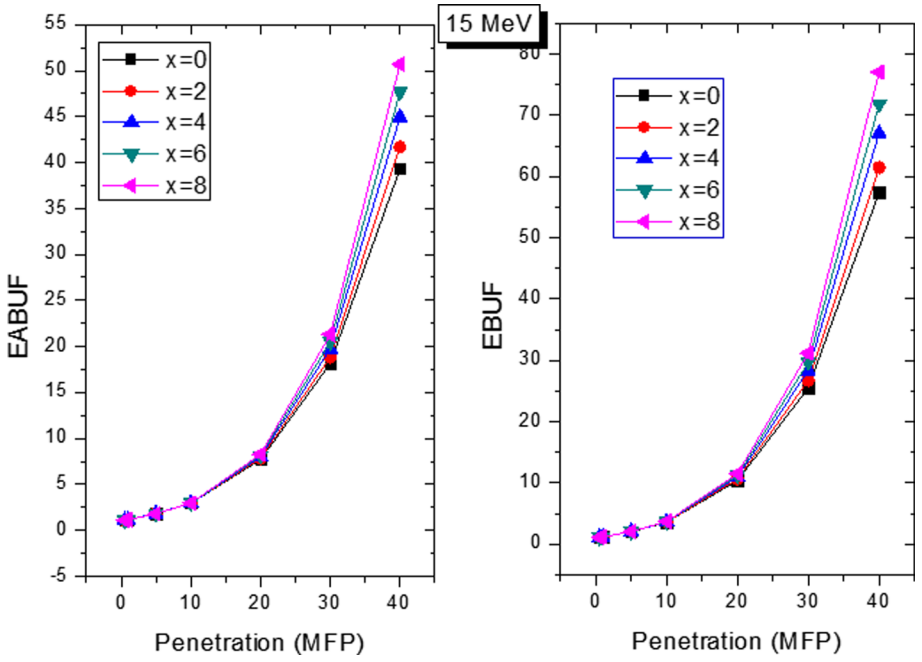

Fig. 15 EABUF and EBUF as a function of depth at 15 MeV for the glasses

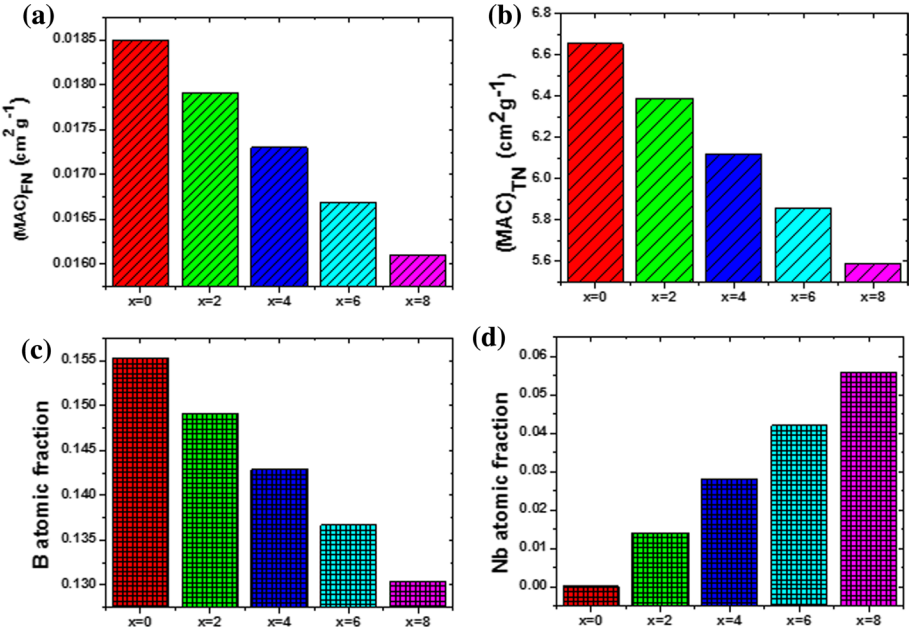

Fig. 16 $(MAC)_{FN}$ **a**, $(MAC)_{TN}$ **b**, atomic fraction of B **c** and Nb **d** in the glasses

3.3.2 Neutrons

The neutron shielding capacity of the glasses were accessed via their mass attenuation coefficient for fast $(MAC)_{FN}$ and thermal $(MAC)_{TN}$ neutrons. The trend in $(MAC)_{FN}$ and $(MAC)_{TN}$ for the glasses is depicted in Fig. 16a and b respectively. A consistent decrease in both parameters is apparent; while $(MAC)_{FN}$ decreased from 0.0185 – 0.0161 cm^2/g, $(MAC)_{TN}$ decayed from 6.6538 – 5.5903 cm^2/g. This trend is enforced by the chemical composition of the glasses. Fast and thermal neutron attenuation is dictated by scattering and absorption cross sections of the chemical constituents of the absorbers (glasses). The relative decline in the atomic fraction of B (0.1553–0.1304) and the corresponding increase in the atomic fraction of Nb (0–0.0592) as shown in Fig. 16c and d, respectively to a large extend is responsible for the trend of both $(MAC)_{FN}$ and $(MAC)_{TN.}$ The scattering and absorption cross sections of B > > that of Nb, hence, the observed trend in the $(MAC)_{FN}$ and $(MAC)_{TN}$ of the investigated glasses. It can therefore be concluded that the increase in the Nb_2O_5 content of the glass system at the detriment of B_2O_5 concentration, has a negative impact on their fast and thermal neutron shielding ability.

3.3.3 Beta particles

The relative beta particle (β) shielding prowess of the glasses was investigated via the total mass stopping power (TSP) and CSDA range of electrons in them. Figure 17 shows the energy dependence of these parameters. The behavior of the TSP is due to the TSP due to energy dependence of radiation and collision energy losses by the electrons (Rammah et al. 2020).

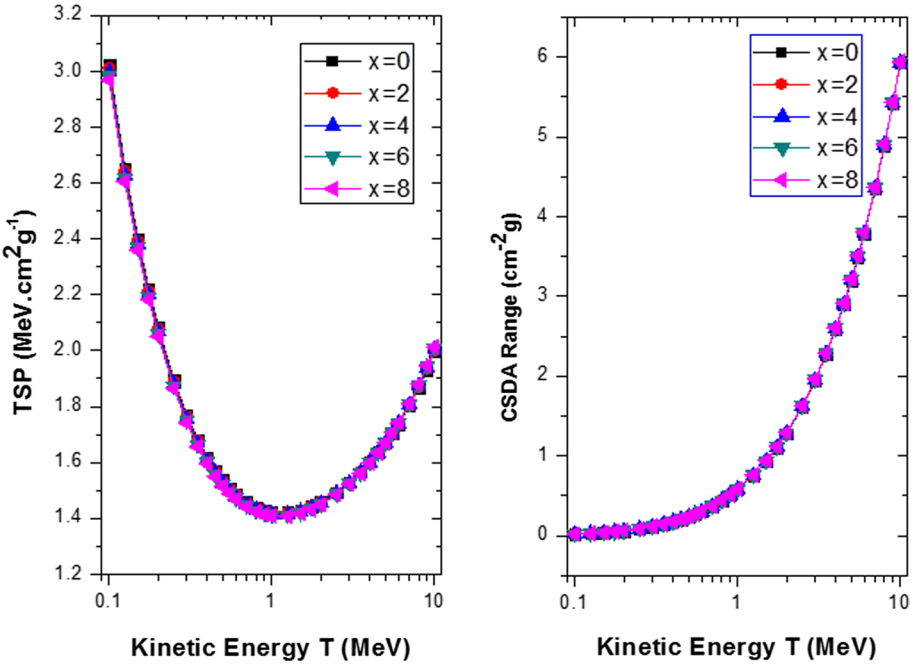

Fig. 17 Total mass stopping power and CSDA range of electrons in the glasses

Analysis of the TSP and CSDA range of the glasses emphasize the fact that there is no significant difference in the charged particle of the glasses irrespective of the weight fraction of Nb_2O_5 relative B_2O_3.

4 Conclusion

Through this work, the physical, optical properties, and radiation shielding parameters of the prepared $(50\text{-}x)B_2O_3 + 30PbO + 10Na_2O + 10MgO + xNb_2O_5$ glasses with various doping ratios x = 0, 2, 4, 6, 8 mol% have been investigated. Glasses were prepared using the well-known melt quenching process and coded as their corresponding x value. The density and molar volume of the prepared glasses were increased from 4.71 g/cm^3 and 23.76 cm^3/mol for the sample with free Nb_2O_5 to 4.91 g/cm^3 and 25.99 cm^3/mol for the rich sample with x = 8 mol% of Nb_2O_5. The broad near-visible band centered was moved towards higher wavelength with increasing Nb_2O_5 content. The predicted direct band gap energies of glass samples felt from 3.728 to 2.939 eV, while the indirect band gap energies from 3.032 to 1.822 eV as the Nb_2O_5 substitution ratio increased. Urbach's energies of the prepared samples were increased with the increasing of Nb_2O_5, indicating less stability and homogeneity materials with more defects, as well as an increase in disorder in the produced glass samples. For photons, the maximum MAC values of 32.67, 33.02, 33.38, 33.74, and 34.10 cm^2/g were recorded for x = 0 – x = 8, respectively at 0.015 MeV, while the least corresponding MAC value of 0.0286, 0.0288, 0.0291, 0.0293, and 0.0295 cm^2/g was obtained at 10 MeV. Maximum and least values of LAC obtained at 15 keV

and 10 MeV corresponds to 154 and 0.134; 157.49 and 0.138; 160.43 and 0.140; 163.60 and 0.142; and 167.51 and 0.145 cm^{-1} for x = 0 – x = 8, accordingly. The Z_{eff} value varies from 10.18 – 32.05 with maximum (minimum) value obtained at 0. 1 and 1.5 MeV. At Pb absorption edge, Z_{eff} = 30.45, 30.70, 30.96, 31.55, and 32.05 for x = 0 – x = 8, accordingly. Clearly, the photon absorption capacity trend of the glasses is such that: x = 0 < x = 2 < x = 4 < x = 6 < x = 8; similar to both LAC and MAC. For neutrons, the fast $(MAC)_{FN}$ was decreased from 0.0185 – 0.0161 cm^2/g, while the thermal $(MAC)_{TN}$ was decayed from 6.6538 – 5.5903 cm^2/g. Results confirm that the current glasses are superior for radiation shielding materials compared to some commercial concrete (OC, HSC, and BMC). The present findings of optical and radiation shielding properties of the current glasses confirm that these glasses can be used to block ultraviolet (UV) radiation and used as a barrier against the transmission of radiation. Also, can be used as fixed windows and fixed barriers in hospitals, mobile panels, and in research laboratories. In addition, the current glasses can be used as shields of fast and thermal neutrons.

Acknowledgements The authors express their gratitude to Princess Nourah bint Abdulrahman, University Researchers Supporting Project (Grant No. PNURSP2022R60), Princess Nourah bint Abdulrahman University, Riyadh, Saudi Arabia.

Author Contribution All authors contribute in Conceptualization, Methodology, Software, Validation, Investigation, Data Curation, Writing-Review and Editing, Visualization.

Data Availability Statements This manuscript contains no additional associated data. All data include in this study are available upon request by contact with the corresponding author.

Declarations

Conflict of interest Authors declare that this manuscript is original, has not been published before, and is not currently being considered for publication elsewhere. The authors declare that they have no conflict of interest.

References

Abouhaswa, A.S., Olarinoye, I.O., Kudrevatykh, N.V., Ahmed, E.M., Rammah, Y.S.: Bi_2O_3 reinforced B_2O_3 + Sb_2O_3 + Li_2O: composition, physical, linear optical characteristics, and photon attenuation capacity. J. Mater. Sci. Mater. Electron. **32**, 12439–12452 (2021)

Abouhaswa, A.S., Rammah, Y.S., Ibrahim, S.E., El-Hamalawy, A.A.: Structural, optical, and electrical characterization of borate glasses doped with SnO_2. J. Non-Cryst. Solids **494**, 59–65 (2018)

Abouhaswa, A.S., Rammah, Y.S., Ibrahim, S.E., El-Mallawany, R.: Optical and electrical properties of lead borate glasses. J. Electron. Mater. **48**, 5624–5631 (2019)

Al-Buriahi, M.S., Olarinoye, I.O., Alomairy, S., Kebaili, I., Kaya, R., Arslan, H., Tonguc, B.T.: Dense and environment friendly bismuth barium telluroborate glasses for nuclear protection applications. Prog. Nucl. Energy **137**, 103763–103769 (2021). https://doi.org/10.1016/j.pnucene.2021.103763

Al-Harbi, N., Sayyed, M.I., Kumar, A., Mahmoud, K.A., Olarinoye, O.I., Alhuthali, A.M.S., Al-Hadeethi, Y.: A comprehensive investigation on the role of PbO in the structural and radiation shielding attribute of P_2O_5–CaO–Na_2O–K_2O–PbO glass system. J. Mater. Sci. Mater. Electron. **32**, 12371–12382 (2021)

Almuqrin, A.H., Albarzan, B., Olarinoye, O.I., Kumar, A., Alwadai, N., Sayyed, M.I.: Mechanical and gamma ray absorption behavior of PbO–WO_3–Na_2O–MgO–B_2O_3 glasses in the low energy range. Materials **14**(13), 3466–3478 (2021). https://doi.org/10.3390/ma14133466

Bashter, I.I.: Calculation of radiation attenuation coefficients for shielding concretes. Ann. Nucl. Energy **24**(17), 1389–2140 (1997)

Berger, M., Coursey, J., Zucker, M.: ESTAR, PSTAR, and ASTAR: Computer Programs for Calculating Stopping-Power and Range Tables for Electrons, Protons, and Helium Ions (version 1.21), http://physics.nist.gov/Star, 1999, [online], http://physics.nist.gov/Star (Accessed June 27, 2021)

Cardinal, T., Fargin, E., Couzi, M., Canioni, L., Segonds, P., Sarger, L., Ducasse, A., Adamietz, F.: Non-linear optical properties of some niobium (V) oxide glasses. Eur. J. Solid State Inorg. Chem. **33**, 597–605 (1996). https://doi.org/10.1002/chin.199644010

Davis, E.A., Mott, N.F.: Conduction in non-crystalline systems V. Conductivity, optical absorption and photoconductivity in amorphous semiconductors. Philos. Mag. J. Theor. Exp. Appl. Phys. **22**(179), 0903–0922 (1970)

Ersundu, A.E., Çelikbilek, M., Aydin, S.: Characterization of B_2O3 and/or WO_3 containing tellurite glasses. J. Non-Cryst. Solids **358**, 641–647 (2012)

Flambard, A., Videau, J.J., Delevoye, L., Cardinal, T., Labrugère, C., Rivero, C.A., Couzi, M., Montagne, L.: Structure and nonlinear optical properties of sodium–niobium phosphate glasses. J. Non-Cryst. Solids **354**, 3540–3547 (2008). https://doi.org/10.1016/j.jnoncrysol.2008.03.017

Gerward, L., Guilbert, N., Jensen, K.B., Levring, H.: X-ray absorption in matter. Reengineering XCOM. Radiat. Phys. Chem. **60**(1–2), 23–24 (2001). https://doi.org/10.1016/S0969-806X(00)00324-8

Gökçe, H.S., Güngör, O., Yılmaz, H.: An online software to simulate the shielding properties of materials for neutrons and photons: NGCal. Radiat. Phys. Chem. **185**, 109519–109524 (2021). https://doi.org/10.1016/j.radphyschem.2021.109519

Harima, Y.: An historical review and current status of buildup factor calculations and applications. Radiat. Phys. Chem. **41**(4–5), 631–672 (1993). https://doi.org/10.1016/0969-806X(93)90317-N

Koudelka, L., Kalenda, P., Mošner, P., Montagne, L., Revel, B.: Structure-property relationship in borophosphate glasses modified with niobium oxide. J. Non-Cryst. Solids **437**, 64–71 (2016)

Mahmoud, K.A., El-Agawany, F.I., Tashlykov, O.L., Ahmed, E.M., Rammah, Y.S.: The influence of BaO on the mechanical and gamma/fast neutron shielding properties of lead phosphate glasses. Nucl. Eng. Technol. **53**, 3816–3823 (2021)

Manohara, S.R., Hanagodimath, S.M., Thind, K.S., Gerward, L.: On the effective atomic number and electron density: a comprehensive set of formulas for all types of materials and energies above 1 keV. Nucl. Instrum. Methods Phys. Res. Sect. B Beam Interact. Mater. Atoms **266**(18), 3906–3912 (2008)

Marcondes, L.M., Maestri, S., Sousa, B., Gonçalves, R., Cassanjes, F.C., Poirier, G.Y.: High niobium oxide content in germinate glasses: thermal, structural and optical properties. J. Am. Ceram. Soc. **101**, 220–230 (2018)

Nowak, N., Cardinal, T., Adamietz, F., Dussauze, M., Rodruguez, V., Durivault-Reymond, L., Deneuvilliers, C., Poirier, J.-E.: Influence of niobium and titanium on optical and physicochemical properties of silicate glasses. Mater. Res. Bull. **48**, 1376–1380 (2013)

Olarinoye, I.: Variation of effective atomic numbers of some thermoluminescence and phantom materials with photon energies. Res. J. Chem. Sci. **1**(2), 64–69 (2011)

Olarinoye, I.O., Odiaga, R.I., Paul, S.: EXABCal: a program for calculating photon exposure and energy absorption buildup factors. Heliyon **5**(7), e02017 (2019). https://doi.org/10.1016/j.heliyon.2019.e02017

Rammah, Y.S., Gaafar, M.S., Marzouk, S.Y., ElRashidy, H., Olarinoye, I.O., El-Mallawany, R.: Ultrasonic waves, mechanical properties and radiation shielding competence of Er^{3+} doped lead borate glasses: experimental and theoretical investigations. J. Aust. Ceram. Soc. **57**, 1163–1176 (2021b)

Rammah, Y.S., Olarinoye, I.O., El-Agawany, F.I., El-Adawy, A.: Environment friendly La^{3+} ions doped phosphate glasses/glass-ceramics for gamma radiation shielding: Their potential in nuclear safety applications. Ceram. Int. **46**(17), 27616–27626 (2020). https://doi.org/10.1016/j.ceramint.2020.07.256

Rammah, Y.S., Olarinoye, I.O., El-Agawany, F.I., El-Adawy, A.: Photon, proton, and neutron shielding capacity of optical tellurite-vanadate glass systems: theoretical investigation. Radiat. Phys. Chem. **184**, 109443 (2021a). https://doi.org/10.1016/j.radphyschem.2021.109443

Rammah, Y.S., Tekin, H.O., Sriwunkum, C., Olarinoye, I., Amani Alalawi, M.S., Al-Buriahi, T.N., Tonguc, B.T.: Investigations on borate glasses within SBC-Bx system for gamma-ray shielding applications. Nucl. Eng. Technol. **53**, 282–293 (2021c)

Sabry, A.I., El-Samanoudy, M.M.: Optical, infrared and electrical conductivity of glasses in the TeO_2–B_2O_3 system. J. Mater. Sci. **30**, 3930–3935 (1995)

Sekhar, K.C., Hameed, A., Narsimlu, N., Alzahrani, J.S., Alothman, M.A., Olarinoye, I.O., Al-Buriahi, M.S., Shareefuddin, M.: Synthesis, optical, structural, and radiation transmission properties of PbO/Bi_2O_3/B_2O_3/Fe_2O_3 glasses: an experimental and in silico study. Opt. Mater. **117**, 111173–111183 (2021). https://doi.org/10.1016/j.optmat.2021.111173

Shams, A.M., Issa, M.R., Hesham, M.H., Zakaly, H.O., Tekin, A.S., Abouhaswa,: Nb_2O_5-Li_2O-Bi_2O_3-B_2O_3 novel glassy system: evaluation of optical, mechanical, and gamma shielding parameters. J. Mater. Sci. Mater. Electron. **31**, 22039–22056 (2020)

Singh, V.P., Badiger, N.M.: Shielding efficiency of lead borate and nickel borate glasses for gamma rays and neutrons. Glass Phys. Chem. **41**(3), 276–283 (2015)

Singh, V.P., Badiger, N.M., Kaewkhao, J.: Radiation shielding competence of silicate and borate heavy metal oxide glasses: comparative study. J. Non-Cryst. Solids **404**, 167–173 (2014)

Şakar, E., Özpolat, Ö.F., Alım, B., Sayyed, M.I., Kurudirek, M.: Phy-X/PSD: development of a user friendly online software for calculation of parameters relevant to radiation shielding and dosimetry. Radiat. Phys. Chem. **166**, 108496–108507 (2020)

Upender, G., Prasad, M.: Raman, FTIR, thermal and optical properties of TeO_2–Nb_2O_5–B_2O_3–V_2O_5 quaternary glass system. J. Taibah Univ. Sci. **11**(4), 583–592 (2017)

Urbach, F.: The long-wavelength edge of photographic sensitivity and of the electronic Absorption of Solids [8]. Phys. Rev. (1953). https://doi.org/10.1103/PhysRev.92.1324

Authors and Affiliations

Norah A. M. Alsaif[1] · Y. S. Rammah[2] · I. O. Olarinoye[3] · Emad M. Ahmed[4] · A. S. Abouhaswa[2,5]

[1] Department of Physics, College of Science, Princess Nourah Bint Abdulrahman University, Riyadh, Saudi Arabia

[2] Department of Physics, Faculty of Science, Menoufia University, Shebin El-Koom, Menoufia 32511, Egypt

[3] Department of Physics, School of Physical Sciences, Federal University of Technology, Minna, Nigeria

[4] Department of Physics, College of Science, Taif University, P.O. Box 11099, Taif 21944, Saudi Arabia

[5] Ural Federal University, Sverdlovskaya oblast, Yekaterinburg, Russia 620002

Terms and Conditions

Springer Nature journal content, brought to you courtesy of Springer Nature Customer Service Center GmbH ("Springer Nature").

Springer Nature supports a reasonable amount of sharing of research papers by authors, subscribers and authorised users ("Users"), for small-scale personal, non-commercial use provided that all copyright, trade and service marks and other proprietary notices are maintained. By accessing, sharing, receiving or otherwise using the Springer Nature journal content you agree to these terms of use ("Terms"). For these purposes, Springer Nature considers academic use (by researchers and students) to be non-commercial.

These Terms are supplementary and will apply in addition to any applicable website terms and conditions, a relevant site licence or a personal subscription. These Terms will prevail over any conflict or ambiguity with regards to the relevant terms, a site licence or a personal subscription (to the extent of the conflict or ambiguity only). For Creative Commons-licensed articles, the terms of the Creative Commons license used will apply.

We collect and use personal data to provide access to the Springer Nature journal content. We may also use these personal data internally within ResearchGate and Springer Nature and as agreed share it, in an anonymised way, for purposes of tracking, analysis and reporting. We will not otherwise disclose your personal data outside the ResearchGate or the Springer Nature group of companies unless we have your permission as detailed in the Privacy Policy.

While Users may use the Springer Nature journal content for small scale, personal non-commercial use, it is important to note that Users may not:

1. use such content for the purpose of providing other users with access on a regular or large scale basis or as a means to circumvent access control;
2. use such content where to do so would be considered a criminal or statutory offence in any jurisdiction, or gives rise to civil liability, or is otherwise unlawful;
3. falsely or misleadingly imply or suggest endorsement, approval , sponsorship, or association unless explicitly agreed to by Springer Nature in writing;
4. use bots or other automated methods to access the content or redirect messages
5. override any security feature or exclusionary protocol; or
6. share the content in order to create substitute for Springer Nature products or services or a systematic database of Springer Nature journal content.

In line with the restriction against commercial use, Springer Nature does not permit the creation of a product or service that creates revenue, royalties, rent or income from our content or its inclusion as part of a paid for service or for other commercial gain. Springer Nature journal content cannot be used for inter-library loans and librarians may not upload Springer Nature journal content on a large scale into their, or any other, institutional repository.

These terms of use are reviewed regularly and may be amended at any time. Springer Nature is not obligated to publish any information or content on this website and may remove it or features or functionality at our sole discretion, at any time with or without notice. Springer Nature may revoke this licence to you at any time and remove access to any copies of the Springer Nature journal content which have been saved.

To the fullest extent permitted by law, Springer Nature makes no warranties, representations or guarantees to Users, either express or implied with respect to the Springer nature journal content and all parties disclaim and waive any implied warranties or warranties imposed by law, including merchantability or fitness for any particular purpose.

Please note that these rights do not automatically extend to content, data or other material published by Springer Nature that may be licensed from third parties.

If you would like to use or distribute our Springer Nature journal content to a wider audience or on a regular basis or in any other manner not expressly permitted by these Terms, please contact Springer Nature at

onlineservice@springernature.com